AJNR

The Role of Ferumoxytol-Enhanced MR Venography in Transvenous Embolization of Cerebrospinal Fluid-Venous Fistulas

Javier L. Galvan, Theodore W. Hagens, Rola Saouaf, Wouter I. Schievink and Marcel M. Maya

AJNR Am J Neuroradiol published online 16 May 2025
http://www.ajnr.org/content/early/2025/05/16/ajnr.A8837

ORIGINAL RESEARCH

The Role of Ferumoxytol-Enhanced MR Venography in Transvenous Embolization of Cerebrospinal Fluid-Venous Fistulas

Javier L. Galvan, Theodore W. Hagens, Rola Saouaf, Wouter I. Schievink and Marcel M. Maya

ABSTRACT

BACKGROUND: Spontaneous intracranial hypotension (SIH) often results from cerebrospinal fluid-venous fistulas (CVFs), and transvenous embolization is an effective treatment. Precise preprocedural venous mapping is crucial to optimize outcomes and mitigate risks.

PURPOSE: To evaluate the utility of Ferumoxytol-enhanced MR venography (MRV) in delineating venous anatomy for preprocedural planning in CVF treatment.

MATERIALS AND METHODS: This retrospective study included 57 participants referred for paraspinal venous embolization between July 2021 and February 2024. Participants were categorized into three groups: SIH with confirmed CVFs, SIH without identified CVFs, and behavioral variant frontotemporal dementia (bvFTD) without CVFs. All participants underwent Ferumoxytol-enhanced MRV to assess venous anatomy.

RESULTS: The cohort had mean age of 56.4 years (range, 18-86 years) and included 31 women and 26 men. Identified findings included a high prevalence of lumbar segmental veins draining directly into the inferior vena cava (93%), lumbar segmental veins draining into the left renal vein (54%), and incomplete ascending lumbar veins (63%). Other findings included a duplicated inferior vena cava (1.8%) and the pathological condition azygos vein stenosis (7%). Preprocedural MRV effectively identified venous variations, guiding tailored intervention strategies, and minimizing procedural risks.

CONCLUSIONS: Ferumoxytol-enhanced MRV provides comprehensive venous mapping, facilitating safer and more efficient planning for CVF treatment.

ABBREVIATIONS: bvFTD = behavioral variant frontotemporal dementia; CTM = CT myelography; CVF(s) = cerebrospinal fluid-venous fistula(s); DSM = digital subtraction myelography; FS = fat saturated; SIH = spontaneous intracranial hypotension; VIBE = volumetric interpolated breath-hold.

Received March 11, 2025; accepted after revision May 05, 2025.
From the Department of Imaging (J.L.G., T.W.H., R.S., M.M.M.) and Neurosurgery (W.I.S.), Cedars-Sinai Medical Center, Los Angeles, CA, USA;.

The authors declare no conflicts of interest related to the content of this article.

Please address correspondence to Marcel M. Maya, MD, Department of Imaging, Cedars-Sinai, 8700 Beverly Blvd M-335, Los Angeles, CA 90048, USA; e-mail: Marcel.Maya@cshs.org.

SUMMARY SECTION

PREVIOUS LITERATURE: Spontaneous intracranial hypotension (SIH) is often caused by cerebrospinal fluid-venous fistulas (CVFs) and transvenous embolization has become a primary minimally invasive treatment. Ferumoxytol-enhanced MR venography (MRV) has emerged as a valuable tool for detailed venous mapping due to its prolonged intravascular retention and ability to visualize complex spinal venous anatomy without radiation.

KEY FINDINGS: Spinal venous anatomy in this SIH cohort showed substantial variability, particularly in the upper thoracic and lumbar regions. Preprocedural MRV effectively identified these variations, guiding tailored embolization approaches and revealing unexpected findings like azygos stenosis.

KNOWLEDGE ADVANCEMENT: This study underscores the crucial role of Ferumoxytol-enhanced MRV for comprehensive preprocedural planning in CVF embolization. It emphasizes the high frequency and clinical relevance of spinal venous anatomical variations, demonstrating how detailed MRV can optimize treatment strategies and potentially improve patient outcomes.

INTRODUCTION

Spontaneous intracranial hypotension (SIH) is a debilitating condition most commonly characterized by orthostatic headaches.[1,2] This condition stems from low cerebrospinal fluid (CSF) volume, typically caused by a spontaneous CSF leak.[3] Spinal CSF leaks are categorized into four types: dural tears (type 1), meningeal diverticulum (type 2), CSF-venous fistula (type 3), and CSF leaks of indeterminate origin

Copyright 2025 by American Society of Neuroradiology.

(type 4).[4] Among these, CSF-venous fistulas (CVF) have gained increasing recognition since their first description as a distinct and treatable cause of SIH.[5,6]

Imaging is integral to the diagnosis and management of SIH. Techniques such as CT myelography (CTM), dynamic CTM, brain MR with and without contrast, spinal MR with myelography and digital subtraction myelography (DSM) performed prone or in the lateral decubitus position are employed to localize and characterize CSF leaks.[7] Treatment options for CVF encompass epidural blood patching, percutaneous fibrin glue injection, venous fistula embolization, and surgical intervention.[6,8,9] Transvenous embolization, occluding the venous fistula via catheter-delivered embolic agents, has emerged as an effective and minimally invasive option, although it is not without risks. Complications, including rebound intracranial hypertension, paraspinal vein perforation, and embolic events, are rare but notable.[2,10]

Accurate preprocedural venous mapping is crucial for optimizing transvenous embolization outcomes. Ferumoxytol-enhanced (Feraheme; Covis Pharmaceuticals) MR venography (MRV) has demonstrated utility in evaluating venous anatomy, particularly in patients with chronic central venous occlusion and evaluating central venous stenosis or occlusion in patients with renal impairment or contraindications to gadolinium-based contrast agents.[11-14] Ferumoxytol's prolonged intravascular retention and lack of dependence on bolus timing enable comprehensive venous imaging over a large field of view, essential for assessing spinal venous anatomy. Additionally, Ferumoxytol-enhanced MRV avoids ionizing radiation, offering a safer alternative for younger or radiation-sensitive populations. These attributes are particularly advantageous when compared to CT venography and gadolinium-based MR venography; both depend on precise bolus timing influenced by factors like patient cardiac function and injection technique, and CT venography also requires radiation.

Technical challenges in transvenous embolization persist, particularly in navigating anatomical variations within the venous system in patients who have not undergone preprocedural Ferumoxytol-enhanced MRV. We hypothesize that preprocedural Ferumoxytol-enhanced MRV will effectively delineate venous anatomy and improve procedural planning, treatment efficiency, and safety. The purpose of this study is to evaluate the utility of Ferumoxytol-enhanced MRV in preprocedural evaluation of CVF treatment and to explore anatomical variations that may impact procedural success.

MATERIALS AND METHODS

This retrospective cohort study was conducted at Cedars-Sinai Medical Center, Los Angeles, California, with Institutional Review Board (IRB) approval. Requirement for written informed consent was waived by the IRB. All aspects of the study were HIPAA-compliant. Starting in January 2001, we began prospectively enrolling all participants with SIH evaluated in person at our institution into a dedicated registry. For this analysis, we utilized this registry to retrospectively examine the medical records and imaging studies of 57 consecutive participants referred to our institution for paraspinal venous embolization from July 2021 to February 2024. Inclusion criteria included participants diagnosed with SIH who underwent MRV with Ferumoxytol for preprocedural evaluation. Exclusion criteria included participants with incomplete imaging studies or contraindications to Ferumoxytol administration. Adherence to the Strengthening the Reporting of Observational Studies in Epidemiology (STROBE) guidelines was maintained, with the checklist included in the supplementary material. This study received no external funding.

Participants were categorized into three groups: (1) those with a diagnosis of SIH and an identified CVF, (2) those with SIH without an identified CVF and (3) those with behavioral variant Frontotemporal Dementia (bvFTD) associated with SIH but no identifiable CVF. Selection bias was minimized by including all consecutive participants meeting the inclusion criteria during the study period. Observer bias was mitigated by independent review of imaging studies by multiple radiologists.

Preprocedural Imaging Protocol

Preprocedural planning for CVF embolization utilized a dedicated MRV protocol. Imaging was performed on either a 1.5T or 3T MRI scanner (Magnetom, Siemens Healthineers) using phased-array head and neck coils and two to three body array coils, adjusted based on patient height. Participants were positioned supine, and craniocaudal coverage extended from the C1 vertebral level to the S1/S2 joint space. Lateral coverage expanded beyond standard sagittal spine imaging to include the inferior vena cava (IVC) and paraspinal venous anatomy. Anteroposterior coverage included the IVC and most spinous processes, with exclusion of some posterior skin.

Imaging sequences included a three-station spine localizer to compose images of the entire spine for vertebral level labeling. This was followed by an axial T1-weighted volumetric interpolated breath-hold (VIBE) fat saturated (FS) sequence (TE: 1.33 ms, TR: 4.06 ms, Flip angle: 9) acquired in three stations. Pre-contrast images were obtained with coronal Angio3D and sagittal Angio3D acquisitions (TE: 0.96 ms, TR: 2.61 ms, FA: 22) in two stations. The pre-contrast axial T1 VIBE FS was acquired to serve as a baseline for post-processing subtraction with the post-contrast axial T1 VIBE FS.

After completion of these pre-contrast sequences, a weighted dose of Ferumoxytol was administered at 0.1 mL/second using an MRI-compatible infusion pump. The Ferumoxytol dose was calculated by multiplying the patient's weight in kilograms by the concentration of Ferumoxytol (4 mg/kg) and then dividing this value by 30. The product of this calculation is the Ferumoxytol dose in milliliters. This dose is then multiplied by 3 to determine the volume of saline required for dilution. Post-contrast imaging consisted of half-dose sagittal Angio3D and full-dose coronal Angio3D acquisitions in two stations, followed by an axial T1 VIBE FS postcontrast sequence. The Angio3D sequence, while often associated with arterial imaging, is a 3D gradient echo sequence that, when used with a pure intravascular contrast agent like Ferumoxytol, depicts both arterial and venous vasculature. Subtraction images and maximum intensity projections of the coronal Angio3D full-dose sequences were generated during post processing.

Image Analysis

Imaging studies were initially interpreted and finalized by a body and cardiovascular MR attending radiologist (R.S.) using Philips Vue PACS (Koninklijke Philips N. V., Amsterdam, NL). Following the application of the study's selection criteria, two radiology residents (J.L.G. and T.W.H.) independently performed a detailed level-by-level review of the finalized MRV studies, focusing on the left and right paraspinal venous anatomy. Subsequently, the residents met with an attending neuroradiologist (M.M.M) for a final review of their findings, leading to a group consensus on the documented anatomical variations. While formal interobserver reliability analysis was not

performed for this retrospective study, the supervision and review process by the experienced neuroradiologist aimed to mitigate potential discrepancies in interpretation. Vertebral levels from the C2 vertebral body to the S1/S2 joint space were identified and labeled using the sagittal localizer.

Level-by-level analysis of the left and right paraspinal venous anatomy was conducted using axial T1 VIBE FS post-contrast images, multiplanar reformats and maximum intensity projections of the Angio3D full-dose subtraction images in the sagittal and coronal planes. Venous anatomy was documented at each spinal level, irrespective of the planned treatment site. MRV findings were correlated with catheter angiography. This evaluation was limited to the angiographically catheterized segments of the paraspinal venous anatomy relevant to the target treatment levels.

Statistical Analysis

Descriptive statistics are reported as N (%) for categorical variables. For normally distributed data, mean ± standard deviation (SD) and range are reported. Statistical analyses were performed (J.L.G. and T.W.H.) using R (version 4.4.2; The R Foundation for Statistical Computing).

RESULTS

From July 26, 2021, to February 22, 2024, a total of 57 participants underwent preprocedural planning using our institution's CVF MRV protocol. The cohort had a mean age of 56.4 years and comprised 31 females (54.4%) and 26 males (45.6%). Regarding diagnoses, 45 participants (78.9%) were diagnosed with CVF, seven participants (12.3%) had SIH without CVF identified, and the remaining five participants (8.8%) were diagnosed with bvFTD. In the CVF cohort, the majority of CVFs were localized in the thoracic spine (56.1%). For classification purposes, cervical CVFs included fistulas in the cervical spine and T1. This classification was based on consideration of T1 as an eloquent nerve root, contributing to the brachial plexus and typically grouped with cervical roots. An additional reason for including T1 fistulas among cervical was our typical angiographic approach that involves accessing the vertebral veins and their tributaries, similar to accessing veins associated with cervical CVFs. In contrast, thoracic CVFs were located from T2-T12, with the typical angiographic access for the right T2-T12 and left T5-T12 levels via the azygos vein and its tributaries. The left T2-T4 levels are generally accessed by catheterizing the left brachiocephalic vein and the left superior intercostal vein. Lumbar CVFs included those in the lumbar and S1 regions. Correlation between the preprocedural MRV findings and subsequent catheter angiography performed for CVF embolization in the 57 participants identified a concordance rate of 96.5%. A detailed summary of baseline participant characteristics is provided in table 1.

Table 1. Baseline Patient Characteristics.

Characteristics	N(%)
Mean (SD) age (years) at embolization	56.4 (14.6 %)
Sex	
Female	31 (54.4%)
Male	26 (45.6%)
Diagnosis	
CSF-Venous Fistula	45 (78.9%)
Cervical	11 (19.3%)
Thoracic	32 (56.1%)
Lumbar	6 (10.5%)
SIH without identified CVF	7 (12.3%)
bvFTD	5 (8.8%)

Subcategories of CSF-venous fistulas are not mutually exclusive. CSF = cerebrospinal fluid. SIH = spontaneous intracranial hypotension.

The most commonly encountered anatomic variation identified on MRV was the presence of one or more lumbar segmental veins draining to the IVC in 53 participants (93%). While the classical anatomical description suggests that lumbar segmental veins typically drain into the ipsilateral ascending lumbar vein, subsequently communicating with the azygos or hemiazygos system, our study found a high prevalence of direct drainage into the IVC. In 31 participants (54.4%), these lumbar segmental veins anastomosed with the left renal vein. Bilateral complete ascending lumbar veins were identified in eight participants (14%), while isolated right and left ascending lumbar veins were observed in four (7%) and nine (15.8%) participants, respectively. Variations in thoracic venous anatomy included a common draining vein of the hemiazygos and accessory hemiazygos veins in 10 participants (17.5%). Less commonly, the hemiazygos and accessory hemiazygos veins drained directly to the left brachiocephalic vein in six (10.5%) and seven (12.3%) participants, respectively. Additional findings included one participant with a duplicated IVC (1.8%), five participants (8.8%) with a midline or left sided azygos vein, and four participants (7.0%) with azygos vein stenosis. Baseline anatomic characteristics are provided in table 2.

Our MRV data revealed that the right upper thoracic levels from T2-T4 primarily drain via the right superior intercostal vein (73.7%), a branch draining to the azygos vein. Upon examining the right T1 level, we observed 56% of cases had a right T1 foraminal vein draining to the right vertebral vein. Similarly, at the left T1, 74% of cases demonstrated that the left T1 foraminal drained to the left vertebral vein rather than the left brachiocephalic vein. Furthermore, substantial anatomical variability was noted for the left T2-T4 levels, with foraminal veins terminating in various sources including the left vertebral (13.5%), left superior intercostal (18.7%), accessory hemiazygos (31.6%) or azygos vein (5.8%). In a large subset of participants (30%), the drainage pathway of the left T2, T3, and T4 segmental veins could not be confidently delineated.

Table 2. Baseline Anatomic Characteristics.

Characteristics	N(%)
Lumbar segmental vein draining into the IVC	53 (93 %)
Lumbar segmental vein draining into the left renal vein	31 (54.4%)
Ascending lumbar vein	
Incomplete	36 (63.2%)
Bilateral	8 (14%)
Right	4 (7.0%)
Left	9 (15.8%)
Common draining vein of the accessory hemiazygos and hemiazygos veins	10 (17.5%
Accessory hemiazygos vein draining to the left brachiocephalic vein	7 (12.3%)
Hemiazygos vein draining to the left brachiocephalic vein	6 (10.5 %)
Midline or left-sized azygos	5 (8.8%)
Duplicated IVC	1 (1.8%)
MRV correlation	55 (95.5%)

DISCUSSION

This study demonstrates the clinical utility of preprocedural MRV with Ferumoxytol for planning transvenous embolization of CVF. While prior studies have characterized the general anatomy of the azygos venous system and its tributaries, classical anatomical descriptions typically outline a relatively consistent pattern. The azygos vein on the right drains the right thoracic spine, with the right superior intercostal vein draining the uppermost aspect (T2-T4) directly into it. On the left, the upper thoracic spine is classically described as draining into the left superior intercostal vein that then drains into the left brachiocephalic vein. The mid thoracic spine (T5-T8) typically drains into the accessory hemiazygos vein, and the lower thoracic spine (T8-T12) drains into the hemiazygos vein. Both the accessory hemiazygos and hemiazygos veins drain into the azygos vein. In the lumbar spine, the classical description involves lumbar segmental veins draining into their respective ascending lumbar veins, subsequently typically draining into the azygos or common iliac vein on the right and the hemiazygos or common iliac vein on the left. However, our findings reveal significant deviations from these textbook descriptions, highlighting the critical need for detailed preprocedural imaging. Foreknowledge of these anatomic variations, made possible through preprocedural MRV, is critical for navigating the complex venous anatomy, improving procedural feasibility and success.

A commonly encountered anatomic characteristic was the presence of a lumbar segmental vein anastomosis with the left renal vein. The prevalence of this finding in our participant population is slightly higher than a previously reported prevalence of 40%.[15] This anastomosis provides an additional access route via the caval system, potentially essential in cases where intersegmental anastomoses through the "conventional" azygos system are insufficient. As previously described by Borg et al, variation within intersegmental vein anastomoses is frequently encountered and may prove problematic during venous target selection for CSF-venous fistula embolization.[16] These challenges are particularly pronounced in the lumbar region, where we observed variability in drainage patterns. Our finding that lumbar segmental veins drain directly into the IVC in a majority of our cases counter its classification as an anatomical variant, however, this pattern differs from the standard description. In the literature, the lumbar segmental veins commonly drain into the ipsilateral ascending lumbar vein.[17] Although a complete ascending lumbar vein facilitates direct access, most of our participants lacked this configuration, instead demonstrating direct drainage from lumbar segmental veins to the IVC and variable intersegmental anastomoses (figure 1). Consequently, accessing lower lumbar segmental veins may require an approach through the IVC, left renal vein, or ipsilateral ascending lumbar veins. This deviation from the classical description underscores the variability in venous anatomy and highlights the importance of individualized preprocedural imaging for planning transvenous interventions.

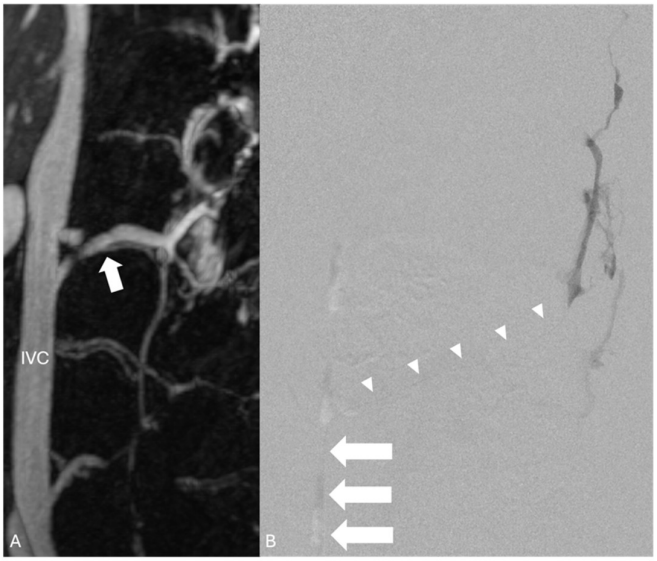

FIG 1 61-year-old female with right L1/2 CSF-venous fistula who underwent preprocedural sagittal MRV (A) that confirmed the right L1 paraspinal vein (white arrow) originating from the IVC. Lateral DSM angiography (B) depicts access to the fistula in the lumbar spine via guide catheter in the IVC (white arrows) and microcatheter in a paraspinal vein (white arrowheads).

In our participant population, upper thoracic venous anatomy exhibited notable variability compared to the standard anatomical descriptions found in the literature.[16,18] For example, previous studies reported the prevalence of accessory hemiazygos-hemiazygos-left

brachiocephalic vein continuation as low as 1-2%, in contrast to the higher frequency in our cohort (figure 2).[19] These variants alter procedural planning, as left-sided paraspinal veins may only be accessed through the caval system necessitating tailored approaches. MRV revealed that in one-third of our cohort, drainage of one or more of the thoracic segmental veins to the azygos vein or its tributaries was not definitively identified or was absent, posing an angiographic challenge as access to the target vein was effectively precluded.

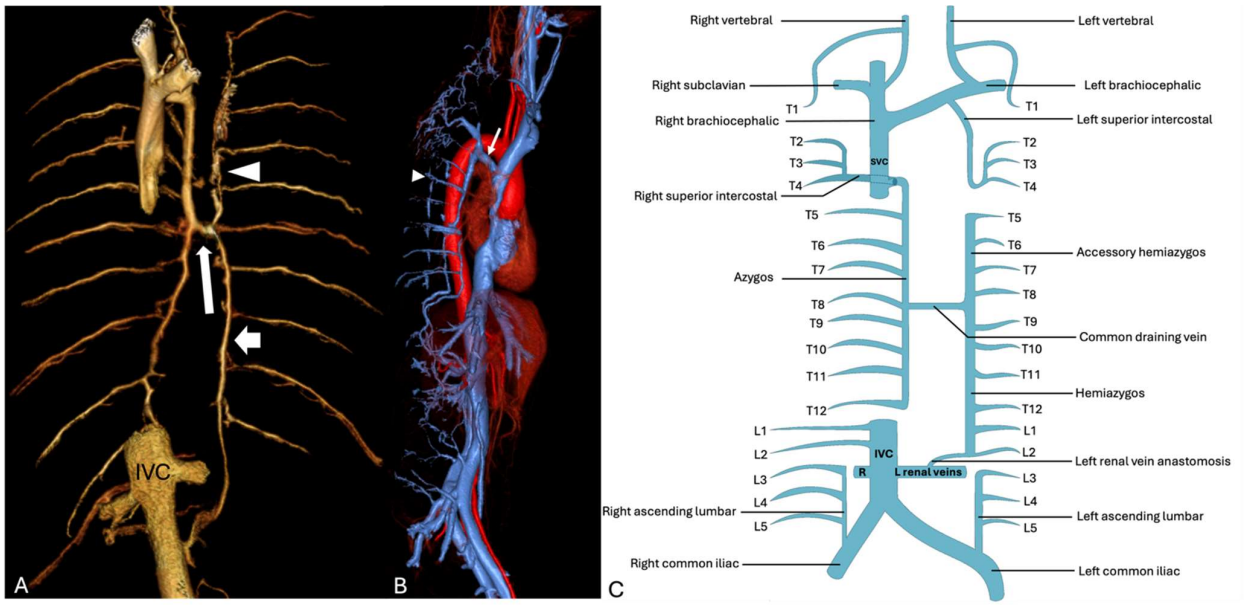

FIG 2 Coronal MRV 3D reconstruction (A) shows a common draining vein (white arrow) for the accessory hemiazygos (arrowhead) and hemiazygos veins (short arrow). Sagittal color 3D reconstruction shows the aortic and venous system with the azygos (white arrow) and paraspinal veins (arrowhead) in profile. Schematic (C) demonstrating a general schematic of the azygos venous system encountered in our cohort (not to scale). Colorized 3D volume rendered rotating cine highlighting both the arterial and venous anatomy is available as a supplemental movie.

Additionally, variations within the azygos vein itself were also observed. Although typically a right-sided structure, several participants in our study had a midline or left-sided azygos vein, occasionally reported in the literature.[16,18] Furthermore, we found a similar prevalence for the hemiazygos and accessory hemiazygos sharing a single draining vein into the azygos vein.[19]

Preprocedural MRV played a pivotal role in identifying azygos vein stenosis, a rare but important finding encountered in four participants in our cohort. This condition has been implicated in SIH and bvFTD. We previously described four participants with azygos vein stenosis who initially presented for embolization; however, preprocedural MRV revealed moderate to high-grade azygos vein stenosis (figure 3). This critical discovery redirected treatment to endovascular stenting of the azygos vein, resulting in prompt symptom improvement in three participants, with remarkable improvement in two and mild improvement in one, underscoring the additional diagnostic and therapeutic value of preprocedural MRV in guiding tailored interventions.[20]

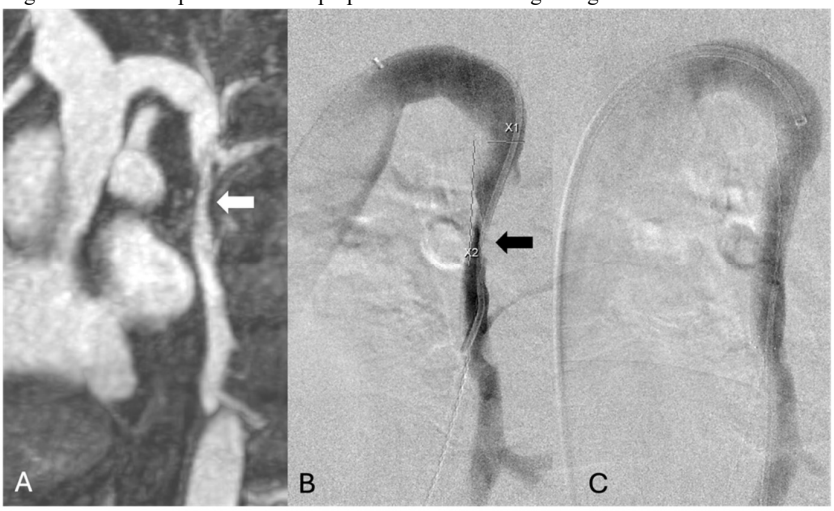

FIG 3 MR-venogram of isolated azygos vein stenosis. Sagittal (A) MRV Feraheme 2D MIP shows azygos vein stenosis (arrow). Lateral angiogram pre-stenting (B) shows azygos stenosis (black arrow). Lateral angiogram post-stenting (C) shows restored flow across the stenosis.

To illustrate the clinical impact of preprocedural MRV, we present the following representative cases where MRV findings influenced

procedural planning and outcomes:

Case 1. A patient with a left T10 CVF had variant azygos anatomy with no communication between the hemiazygos and azygos veins. Instead, the hemiazygos drained into the left brachiocephalic vein (figure 4). This MRV finding allowed modification of the angiographic approach by selectively catheterizing the hemiazygos via the left brachiocephalic vein, enabling successful embolization.

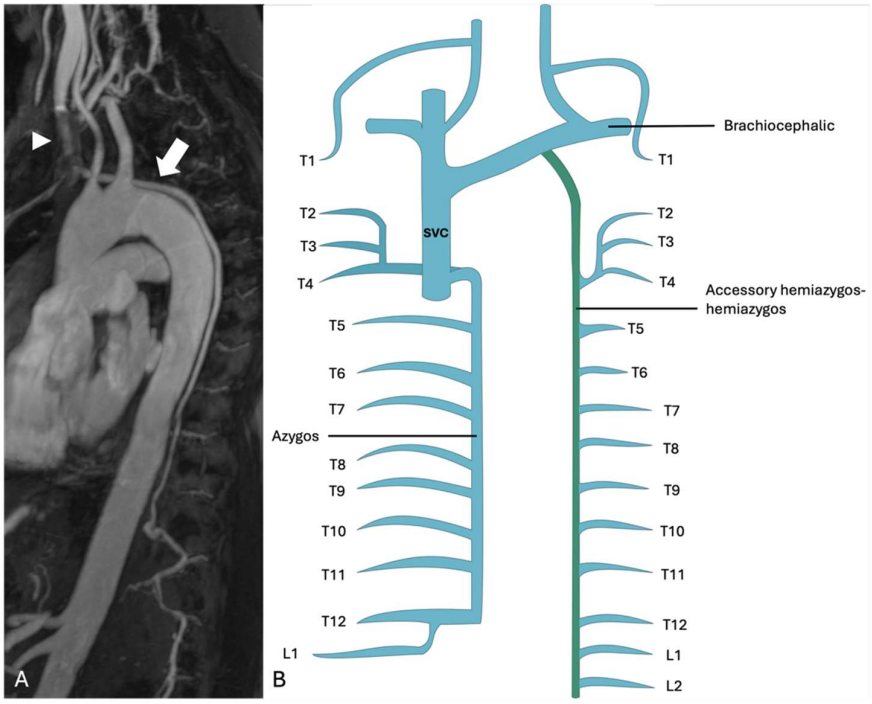

FIG 4 58-year-old female with left T10 CSF-venous fistula who underwent preprocedural sagittal MRV 3D MIP (A) demonstrating hemiazygos vein (arrow) draining directly into the left brachiocephalic vein (arrowhead). Illustration (B) depicting a common accessory hemiazygos-hemiazygos draining into the left brachiocephalic (not to scale).

Case 2. A patient with a left T7 CVF showed no direct communication to the left T7 paraspinal vein via the azygos vein on MRV (figure 5). Subsequent DSA confirmed the absence of direct access, resulting in an unsuccessful procedure.

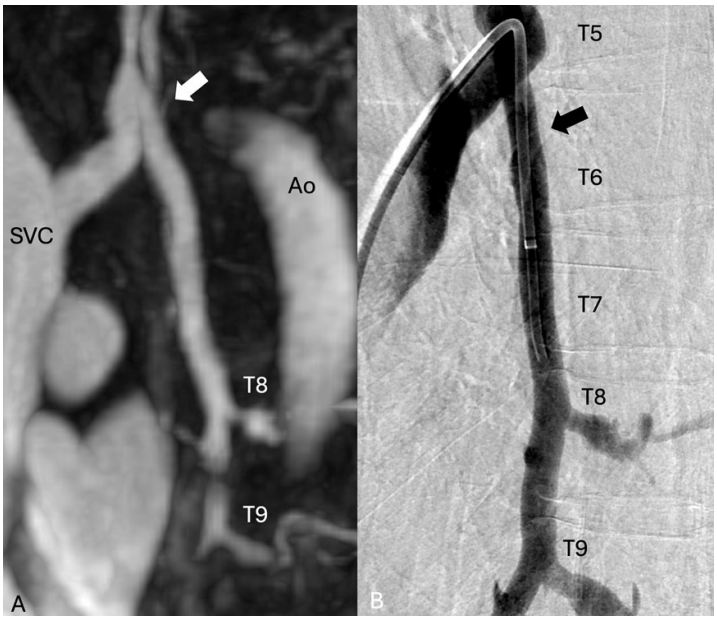

FIG 5 75-year-old female with history of left T7 CSF-venous fistula. Sagittal MRV (A) demonstrates prominent left T8 and T9 paraspinal veins and no paraspinal vein at T7. Lateral angiogram (B) confirms the prominent left T8 and T9 paraspinal veins but no left T7 paraspinal vein. Ao – Aorta, SVC – superior vena cava.

Case 3. A patient with bilateral T11-12 CVF was found to have duplication of the IVC (figure 6). In this patient, the right and left T11 and T12 paraspinal veins drained into their respective ipsilateral caval veins. This required an altered angiographic approach with targeted embolization of the right side via the dominant IVC and targeted embolization of the left side via the duplicated IVC moiety. Recognizing this variant prior to the procedure facilitated successful liquid embolization of the bilateral T11-12 levels by accessing the paraspinal veins through its ipsilateral IVC moiety.

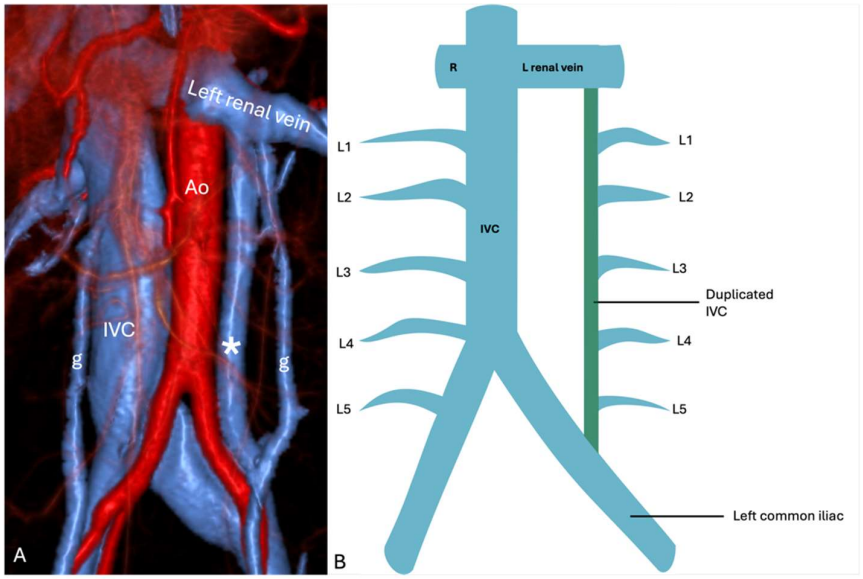

FIG 6 53-year-old female with history of bilateral T11/12 and T12/L1 CSF-venous fistulas. Colorized 3D volume rendered (A) and illustration (B) showing a duplicated IVC (asterisk). Ao – aorta; IVC – inferior vena cava; g – gonadal veins; asterisk - duplicated moiety IVC.

Case 4. A patient with bvFTD, brain sagging on MRI, normal MR-myelography and DSM, and a thoracic calcified disc herniation identified on post-DSM CT underwent evaluation. Thoracic laminectomy failed to reveal a dural defect. However, preoperative MRV demonstrated azygos vein stenosis that was subsequently treated with stenting, resulting in marked improvement in symptomatology (figure 3).

It is important to note that this study largely reflects a highly selected patient group referred to a quaternary center for intracranial hypotension. Second, Ferumoxytol-enhanced MRV is not widely adopted due to its relatively higher cost. Third, the inclusion of five participants with bvFTD and associated SIH but no identifiable CVF may be seen as tangential to the primary focus on preprocedural evaluation for CVF embolization. However, these participants were included as part of the consecutive enrollment of all SIH patients evaluated at our institution during the study period. Furthermore, the identification of azygos vein stenosis in this subgroup, as previously reported, highlights a potential overlapping physiology in some patients presenting with SIH-like symptoms, regardless of the presence of a CVF.[20] While bvFTD group does not directly inform the utility of MRV for CVF embolization planning, its inclusion provides a more comprehensive view of the spectrum of SIH-related conditions encountered in our practice where Ferumoxytol-enhanced MRV was utilized.

An interesting area for future research could involve a more formal comparison of the observed venous anatomy in this patient cohort with that of a control population. However, obtaining a suitable control group of individuals undergoing Ferumoxytol-enhanced MRV for non-SIH indications presents a challenge, as this imaging modality and contrast agent are typically reserved for specific clinical scenarios. Within our study, the non-CVF containing spinal segments in each patient served as an internal reference for assessing anatomical variations, as the presence of a CVF is not expected to inherently alter the overall venous architecture. Future investigations might explore comparisons with established anatomical descriptions or carefully selected control groups if ethically and practically feasible.

CONCLUSIONS

Our study highlights the important role of MRV with Ferumoxytol in preprocedural planning for CSF paraspinal venous embolization. The variability in venous anatomy observed in our cohort emphasizes the importance of detailed preprocedural imaging to optimize procedural success and minimize technical challenges. The identification of key anatomic variants through MRV facilitates tailored procedural approaches, ultimately enhancing patient outcomes in this challenging and evolving field.

REFERENCES

1. Schievink WI. Spontaneous intracranial hypotension. *N Engl J Med*. 2021;385(23):2173. doi: 10.1056/nejmra2101561.
2. Mehta D, Cheema S, Davagnanam I, Matharu M. Diagnosis and treatment evaluation in patients with spontaneous intracranial hypotension. *Frontiers in neurology*. 2023;14:1145949. doi: 10.3389/fneur.2023.1145949.

3. Schievink WI, Deline CR. Headache secondary to intracranial hypotension. *Curr Pain Headache Rep*. 2014;18(11). doi: 10.1007/s11916-014-0457-9.
4. Schievink WI, Maya MM, Jean-Pierre S, Nuño M, Prasad RS, Moser FG. A classification system of spontaneous spinal CSF leaks. *Neurology*. 2016;87(7):673–679.
5. Schievink WI, Moser FG, Maya MM. CSF–venous fistula in spontaneous intracranial hypotension. *Neurology*. 2014;83(5):472–473. doi: 10.1212/WNL.0000000000000639.
6. Brinjikji W, Savastano LE, Atkinson JLD, Garza I, Farb R, Cutsforth-Gregory JK. A novel endovascular therapy for CSF hypotension secondary to CSF-venous fistulas. *AJNR Am J Neuroradiol*. 2021;42(5):882. doi: 10.3174/ajnr.a7014.
7. Galvan J, Maya M, Prasad RS, Wadhwa VS, Schievink W. Spinal cerebrospinal fluid leak localization with digital subtraction myelography. *Radiologic Clinics of North America*. 2024;62(2):321. doi: 10.1016/j.rcl.2023.10.004.
8. Shlobin NA, Shah VN, Chin CT, Dillon WP, Tan LA. Cerebrospinal fluid-venous fistulas: A systematic review and examination of individual patient data. *Neurosurg*. 2021;88(5):931. doi: 10.1093/neuros/nyaa558.
9. Brinjikji W, Garza I, Whealy M, et al. Clinical and imaging outcomes of cerebrospinal fluid-venous fistula embolization. *J NeuroIntervent Surg*. 2022;14(10):953. doi: 10.1136/neurintsurg-2021-018466.
10. Orscelik A, Senol YC, Musmar B, et al. Endovascular embolization of cerebrospinal fluid-venous fistula: A comprehensive systematic review on its efficacy and safety for the management of spontaneous intracranial hypotension. *Neurosurg Rev*. 2024;47(1):28. doi: 10.1007/s10143-023-02264-1.
11. Schwein A, MD, Lu T, MD, Chinnadurai, Ponraj, MBBS, MMST, et al. Magnetic resonance venography and three-dimensional image fusion guidance provide a novel paradigm for endovascular recanalization of chronic central venous occlusion. *Journal of vascular surgery. Venous and lymphatic disorders*. 2017;5(1):60–69. doi: 10.1016/j.jvsv.2016.07.010.
12. Gallo CJR, Mammarappallil JG, Johnson DY, et al. Ferumoxytol-enhanced MR venography of the central veins of the thorax for the evaluation of stenosis and occlusion in patients with renal impairment. *Radiology. Cardiothoracic imaging*. 2020;2(6):e200339. doi: 10.1148/ryct.2020200339.
13. Shahrouki P, Moriarty JM, Khan SN, et al. High resolution, 3-dimensional ferumoxytol-enhanced cardiovascular magnetic resonance venography in central venous occlusion. *Journal of cardiovascular magnetic resonance*. 2019;21(1):17. doi: 10.1186/s12968-019-0528-5.
14. Hope MD, Hope TA, Zhu C, et al. Vascular imaging with ferumoxytol as a contrast agent. *American journal of roentgenology*. 2015;205(3):W366–W373. doi: 10.2214/AJR.15.14534.
15. Kumar S, Neyaz Z, Gupta A. The utility of 64 channel multidetector CT angiography for evaluating the renal vascular anatomy and possible variations: A pictorial essay. *Korean journal of radiology*. 2010;11(3):346–354. doi: 10.3348/kjr.2010.11.3.346.
16. Borg N, Cutsforth-Gregory J, Oushy S, et al. Anatomy of spinal venous drainage for the neurointerventionalist: From puncture site to intervertebral foramen. *AJNR Am J Neuroradiol*. 2022;43(4):517. doi: 10.3174/ajnr.a7409.
17. Gray H, Standring S. *Gray's anatomy. the anatomical basis of clinical practice.* 40th ed. Edinburgh: Elsevier, Churchill Livingstone; 2008:1080–1089.
18. Théron J, Moret J. *Spinal phlebography : Lumbar and cervical techniques.* 1st ed. Berlin, Heidelberg: Springer-Verlag; 1978. 10.1007/978-3-642-95324-8.
19. Panesar H, Singh M, Adams Q, Titunick MB, Pagano AS. Cadaveric dissection of connection between accessory hemiazygos vein and left brachiocephalic vein. *Surg Radiol Anat*. 2023;45(9):1145–1148. doi: 10.1007/s00276-023-03191-y.
20. Schievink WI, Maya MM, Saouaf R, et al. Azygos vein stenosis in frontotemporal dementia sagging brain syndrome. *American journal of neuroradiology : AJNR*. 2025. doi: 10.3174/ajnr.A8532.

SUPPLEMENTAL FILES

Supplemental Table. Imaging Protocol for MR Venography.

Sequence	TA	FoV	Base res	Phase res	Slice th	Slice gap	# of slices	TR	TE	TI	Flip ang	Bandwidth	Fat suppr.
trufi_multiplane _loc thoracic * (tfi)	8.6	400 mm	256	100 %	5.0 mm	100 %	5	3.13 ms	1.57 ms		55 deg	781 Hz/Px	None
SAG LOC 500 FOV * (tse)	0:23	500 mm	512	75 %	4.0 mm	40 %	5	350.0 ms	10 ms		150 deg	168 Hz/Px	None
AX T1 FS VIBE PRE_bh_UPPER * (fl)	0:16	400 mm	320	75 %	3.0 mm	20 %	80	4.41 ms	2.14 ms		10.0 deg	350 Hz/Px	Q-fat sat.
AX T1 FS VIBE PRE_bh_LOWER * (fl)	0:16	400 mm	320	75 %	3.0 mm	20 %	80	4.41 ms	2.14 ms		10.0 deg	350 Hz/Px	Q-fat sat.
Angio3D_cor_pre * (fl)	0:16	500 mm	416	80 %	1.20 mm	20 %	96	3.07 ms	1.05 ms		25 deg	450 Hz/Px	None
Angio3D_sag_pre * (fl)	0:16	500 mm	416	80 %	1.20 mm	20 %	80	3.05 ms	1.04 ms		25 deg	450 Hz/Px	None
Angio3D_cor - HALF DOSE * (fl)	0:16	500 mm	416	80 %	1.20 mm	20 %	96	3.07 ms	1.05 ms		25 deg	450 Hz/Px	None
Angio3D_sag - HALF DOSE * (fl)	0:16	500 mm	416	80 %	1.20 mm	20 %	80	3.05 ms	1.04 ms		25 deg	450 Hz/Px	None
Angio3D_cor - FULL DOSE * (fl)	0:16	500 mm	416	80 %	1.20 mm	20 %	96	3.07 ms	1.05 ms		25 deg	450 Hz/Px	None
Angio3D_sag - FULL DOSE * (fl)	0:16	500 mm	416	80 %	1.20 mm	20 %	80	3.05 ms	1.04 ms		25 deg	450 Hz/Px	None
AX T1 FS VIBE POST_bh_UPPER * (fl)	0:16	400 mm	320	75 %	3.0 mm	20 %	80	4.41 ms	2.14 ms		10.0 deg	350 Hz/Px	Q-fat sat.
AX T1 FS VIBE POST_bh_LOWER * (fl)	0:16	400 mm	320	75 %	3.0 mm	20 %	80	4.41 ms	2.14 ms		10.0 deg	350 Hz/Px	Q-fat sat.

Supplemental Movie. Colorized 3D volume rendered rotating cine highlighting both the arterial and venous anatomy.